JOURNAL OF THE ROYAL SOCIETY Interface

J. R. Soc. Interface (2010) **7**, 603–611
doi:10.1098/rsif.2009.0300
Published online 23 September 2009

Enhancement of natural background gamma-radiation dose around uranium microparticles in the human body

John E. Pattison[1,*], Richard P. Hugtenburg[2] and Stuart Green[3]

[1]*School of EIE—Applied Physics, University of South Australia, Mawson Lakes, South Australia 5095, Australia*
[2]*School of Medicine, University of Swansea, Swansea SA2 8PP, UK*
[3]*Department of Medical Physics, University Hospital Birmingham NHS Trust, Birmingham B15 2TH, UK*

Ongoing controversy surrounds the adverse health effects of the use of depleted uranium (DU) munitions. The biological effects of gamma-radiation arise from the direct or indirect interaction between secondary electrons and the DNA of living cells. The probability of the absorption of X-rays and gamma-rays with energies below about 200 keV by particles of high atomic number is proportional to the third to fourth power of the atomic number. In such a case, the more heavily ionizing low-energy recoil electrons are preferentially produced; these cause dose enhancement in the immediate vicinity of the particles. It has been claimed that upon exposure to naturally occurring background gamma-radiation, particles of DU in the human body would produce dose enhancement by a factor of 500–1000, thereby contributing a significant radiation dose in addition to the dose received from the inherent radioactivity of the DU. In this study, we used the Monte Carlo code EGSnrc to accurately estimate the likely maximum dose enhancement arising from the presence of micrometre-sized uranium particles in the body. We found that although the dose enhancement is significant, of the order of 1–10, it is considerably smaller than that suggested previously.

Keywords: Gulf War syndrome; depleted uranium; photoelectric effect; natural background gamma-radiation; EGSnrc

1. INTRODUCTION

Since the First Gulf War in 1991, controversy has surrounded the adverse health effects of depleted uranium (DU) munitions. Military personnel returning from recent wars in the Middle East and Balkans, where such munitions have been used, have complained of a range of illnesses labelled collectively as 'Gulf War syndrome'. This syndrome has been linked to the ingestion and inhalation of the radioactive combustion products of DU munitions and the presence of DU fragments in shrapnel wounds, among other reasons. The syndrome, along with the possible role of DU in its genesis, has been the subject of a number of high-level reviews undertaken by the International Red Cross (IRC 2001), the World Health Organization (WHO 2001), the Royal Society (2001, 2002) and the US Institute of Medicine (IOM 2006, 2008), as well as large-scale epidemiological studies of veterans undertaken by the US Veterans Affairs and Department of Defence (VADD 2002) and the UK Depleted Uranium Oversight Board (DUOB 2007).

*Author for correspondence (john.pattison@unisa.edu.au).

The above studies discounted any association between DU and the alleged medical problems, reasoning that the very low radiological toxicity of DU and generally low levels of exposure correspond to very low health risks. This general conclusion has been supported by independent researchers in Australia (Sim & Kelsall 2006), Canada (Ough *et al.* 2002), Sweden (Gustavsson *et al.* 2004) and Denmark (Storm *et al.* 2006). Some of the reports did recommend, however, the need for continued surveillance of DU-exposed service personnel, although they uncovered no cluster of symptoms that constitute a syndrome unique to the veterans of the Gulf and Balkan wars (Horn *et al.* 2006).

This finding is not totally surprising, as similar conclusions were found regarding the alleged adverse health effects of the more radioactive small 'hot particles' (with activities of the order of 1–10 mBq)—radioactive contamination from nuclear power plants, atomic bomb test sites, etc. Hot particles may also occur naturally from the weathering of igneous rocks (Hamilton 1988). It was originally argued that radiation exposure arising from small radioactive particles may be

Received 19 July 2009
Accepted 24 August 2009

far more carcinogenic than the case when the same amount of energy is deposited uniformly throughout a tissue volume; however, Charles *et al.* (2003) and Charles & Harrison (2007) found a lack of evidence in support of a large hot-particle enhancement factor for carcinogenesis.

Despite the above findings, protagonists have continued to claim that DU is responsible for a multitude of illnesses. Given the low level of inherent radioactivity of DU particles (of the order of 1–100 μBq) and the correspondingly low doses involved, a number of novel mechanisms have been proposed that might lead to an increase in the received radiation doses and, consequently, the severity of the ensuing health effects. These include the 'second-event' hypothesis (Busby 1998, 2000), which provides a mechanism for an increase in the biological effect of the inherent radioactivity of sequentially decaying internal radionuclides (e.g. ^{90}Sr–^{90}Y) arising from 'sensitizing' of the DNA molecule during a certain phase of the cell cycle. This hypothesis was critically examined by Edwards & Cox (2000) and was found to be unsatisfactory (CERRIE 2004).

The dose-enhancing effect of high-atomic-number particles has also been suggested as a mechanism by which low levels of radiation might lead to adverse health effects. As a mechanism of increasing the radiation dose in the vicinity of DU particles in the body, it has been suggested that the radiation dose to the tissue immediately surrounding DU particles arising from the inherent radioactivity of uranium is complemented by an enhancement in the radiation dose received from the natural background gamma-radiation (and medical X-rays; Busby 2005). This additional dose is enhanced owing to the photoelectric interaction of predominantly low-energy photons in the natural background radiation, below about 200 keV, whereby natural background gamma-rays are converted into short-range photoelectrons by high-atomic-number materials such as uranium. The absorption of low-energy photons owing to the photoelectric effect is proportional to the atomic number to about the third or fourth power.

Employing indirect arguments, based on the differential absorption rates of mono-energetic photons in tissue and uranium, Busby (2005) estimated that this dose enhancement is of the order of a factor of 500–1000 or more (Tickell 2008). For these estimations, Busby considered photon energies less than 200 keV, spherical particles with diameters in the range 0.2–5 μm, and a photoelectron range of 25 μm in tissue. According to this view, an absorbed dose of 1 mGy becomes an absorbed dose of at least 500 mGy in the DU particle; this enhanced dose is then redistributed into the cells close to the DU particle. In addition, for photon energies above about 200 keV, other photon interaction processes (e.g. Compton scattering and pair production; figure 1) eventually result in low-energy photons of which a large fraction is also absorbed and converted to photoelectrons. For most ionizing radiations, a large proportion of the absorbed dose is deposited by low-energy recoil electrons. Photoelectrons generated within DU particles will emerge into the surrounding tissue with reduced energy, thereby having a shorter range and being more strongly ionizing close to the DU particle. These ionizations by photoelectrons are proposed to result in high local doses, causing damage in addition to that produced by the alpha- and beta-emissions of the DU particles themselves.

The occurrence of this enhancement effect is widely accepted: it has been known for some time that the photoelectric effect results in an enhancement of the radiation dose in volumes surrounding high-atomic-number materials. The strong absorption of low-energy photons by high-atomic-number (Z) materials such as iodine ($Z = 53$), barium (56) and bismuth (83) relative to both tissue (7.5) and bone (12) has been used in radiology since about 1905 as a means of enhancing image contrast. The locally enhanced dose around high-atomic-number materials was first suggested for use in radiotherapy by Spiers (1949). Considerable research effort is currently underway to make use of this phenomenon in developing a practical procedure to deliver non-toxic high-atomic-number elements such as iodine (53), gadolinium (64), platinum (78) and gold (79) to tumours before being irradiated, with the aim of selectively enhancing the radiation dose received by the tumour while sparing the surrounding healthy tissue (e.g. Biston *et al.* 2004; Adam *et al.* 2006; De Stasio *et al.* 2006; Hugtenburg *et al.* 2007; Hainfeld *et al.* 2008; Zhang *et al.* 2008).

The suggestion of a dose enhancement of natural background gamma-radiation to cells surrounding DU particles in the human body appears to be feasible, yet no detailed analysis of the phenomenon has been attempted; consequently, the present study was undertaken with the aim of determining the magnitude of the enhancement. This study did not take into account the pathways in which the DU particles entered the body, whether by inhalation, ingestion or by wound contamination, or where or for how long the DU particles remained in the body or the likely subsequent health effects. A preliminary report on this study was published by Pattison *et al.* (2008).

2. MATERIAL AND METHODS

2.1. Natural background gamma-radiation spectrum

The composition and magnitude of natural background gamma-radiation varies widely around the Earth, especially with latitude and altitude. At sea level, it is predominantly due to terrestrial gamma-rays and to lesser degree cosmic-ray-induced gamma-rays. Accordingly, in the present study we analyse five similar measured natural background gamma-radiation pulse-height spectra (three from the USA and two from Europe), as collected using NaI(Tl) detectors of similar size (Lowder *et al.* 1964; Blum *et al.* 1997; Aage *et al.* 1999; Busby 2005; Redus *et al.* 2007). From these spectra, we calculated a single weighted-average spectrum curve (figure 2).

The average pulse-height spectrum is produced by multiple interactions in the NaI(Tl) detector and the surrounding environment by Compton scattering,

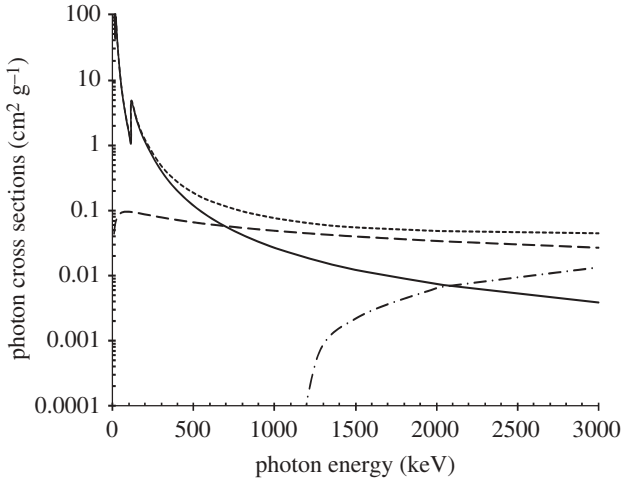

Figure 1. Photon interaction cross sections for uranium as a function of photon energy. Note that the total attenuation below a photon energy of about 200 keV is due nearly entirely to the photoelectric effect. As the photon energy increases above 200 keV, Compton scattering increases until it is the dominant interaction mechanism above about 700 keV. Solid line, PE absorption; dashed line, Compton scatter; dash-dotted line, pair production; dotted line, total attenuation. Adapted from Berger & Hubbell (1987).

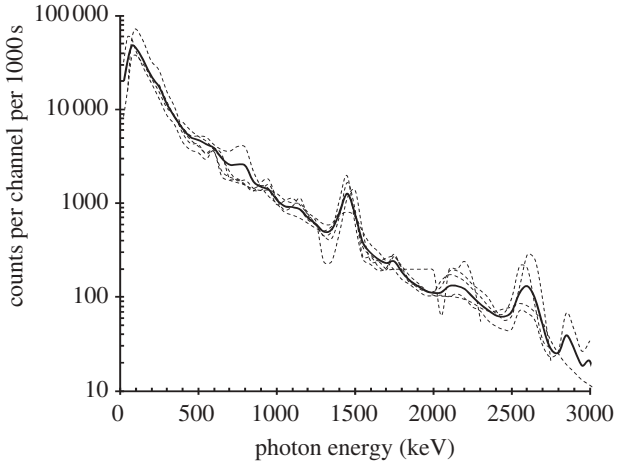

Figure 2. Measured pulse-height spectra using 76 mm × 76 mm cylindrical Na(Tl) crystal with minimum shielding, 256 (12 keV) channels, and 1000 s counting time for five different locations in North America and Europe shown as faint dashed curves. The weighted-average curve is shown as a bold continuous curve.

photoelectric absorption and pair production, with smaller discrete line emissions from ^{40}K and the ^{238}U and ^{232}Th series, most of which blur into the average curve. The characteristic peaks at 1460 keV due to ^{40}K and at 2610 keV due to ^{208}Tl (in the ^{232}Th series) are apparent. The five measured spectra are all similar, within $\pm$33 per cent about the average curve. Other measured natural background gamma-radiation spectra may vary by a greater amount than that indicated by this range. The average curve was then deconvolved using a Monte Carlo model of the NaI detector to give the free-in-air gamma-radiation fluence-rate spectrum incident on the NaI detector (Waters 2002), shown as the solid line in figure 3.

Given that people are in various orientations during the day, both inside and outside buildings, and that the radiation field is quasi-isotropic, this free-in-air gamma-radiation was assumed to be isotropically incident on the outside of the model body under consideration.

2.2. Model body

Neither mathematical-type nor voxel-type body models, which attempt to represent the internal anatomy of the body and are used to estimate organ doses in individuals, were considered appropriate for the 'typical' person considered here. Because of the quasi-isotropic nature of the radiation field and the various orientations of people in the field, the body was modelled as a right circular cylinder for the trunk with a radius of 16 cm and a length of 60 cm. The model body had no head, arms or legs, but a short cylindrical neck (length, 10 cm; radius, 7 cm) and short annular cylindrical thighs (length, 10 cm; outer radius, 16 cm; inner radius for the crutch, 3 cm), thereby retaining the rotational symmetry of the body (figure 4). Given that the scattered radiation from the neck and thighs contributed only about 1 per cent of the dose at the midplane of the trunk, their exact dimensions are not important. But because this scattered radiation contributed extra low-energy photons to the internal photon-fluence spectra on the midplane of the trunk, they were included in the analysis. The trunk dimensions are consistent with the dimensions given in ICRP (2003) for the average typical adult male and female. The model body was assumed to consist of homogeneous ICRU four-element tissue (ICRU 1989), and is comparable with a similar, although slightly smaller, body model used in Pattison *et al.* (2001, 2004).

2.3. Uranium particles

Natural uranium exists as three radioactive isotopes: ^{238}U (half-life, 4.5 Gyr), ^{235}U (710 Myr) and ^{234}U (0.25 Myr), typically in the proportions 99.3, 0.7 and 0.006 per cent by mass, or 48, 2 and 50 per cent by activity, respectively. Natural uranium is only weakly radioactive. DU is mainly a by-product from the chemical enrichment of natural uranium, whereby the fissionable ^{235}U is extracted; it also lacks the decay products of most concern, e.g. radium and polonium. This enrichment process reduces the radioactivity of the remaining DU to about 60 per cent of that of natural uranium. A less-common source is the reprocessing of spent reactor fuel. If the DU is partly derived from reprocessed reactor fuel, then it may also contain ^{236}U (approx. 0.0003%) and smaller amounts of other artificial isotopes (Mitchel & Sunder 2004; Trueman *et al.* 2004). The DU is pyrophoric; that is, when in fine powder form, it spontaneously combusts with about 80 per cent conversion to U_3O_8 and UO_2 (DUOB 2007). As uranium is a heavy metal, similar to mercury and lead, it is also chemically toxic: normal functioning of the kidney, brain, liver and heart can be affected by an excessive exposure to DU (Craft *et al.* 2004).

The sizes and shapes of actual uranium oxide particles have been examined using scanning electron microscopy

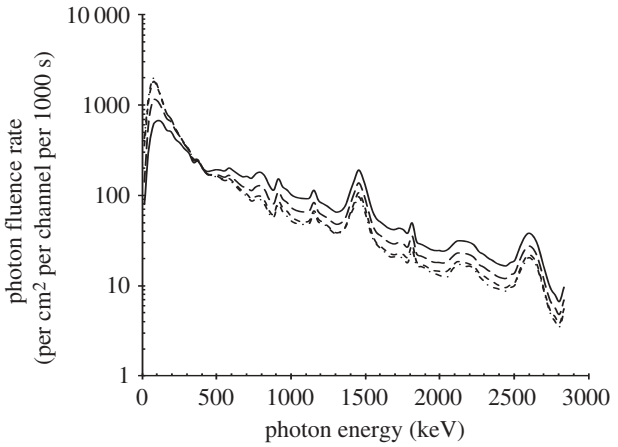

Figure 3. Incident isotropic free-in-air gamma-radiation fluence-rate spectrum, and internal photon fluence-rate spectra. Solid line, incident outside body; long-dashed line, just inside body; small-dashed line, half-way inside body; dashed-dotted line, on axis inside body.

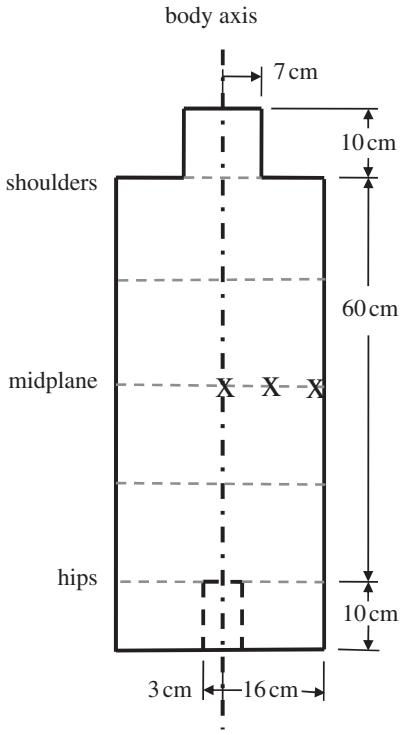

Figure 4. Body (torso) model. The positions on the midplane where the enhancement factors are calculated are shown by 'X'.

by Milodowski (2001) and Salbu *et al.* (2005) for samples collected from battlefields and by Cho *et al.* (2002) for samples prepared in the laboratory. The shapes are highly irregular, with both convex and concave surfaces observed in individual particles, and with a typical size of about 5 μm (Royal Society 2001). Consequently, DU particles were modelled in the present study as small right circular cylinders of two sizes: a small particle of 2 μm in diameter and height, and a large particle of 10 μm in diameter and height (figure 5). Note the existence of three types of surfaces on these cylindrical particles: plane ends, convex sides and double-convex corners. The enhancement factors (dose with the uranium particle present)/(dose without the uranium particle) for each particle size were determined in the vicinity of each of these three surfaces. Given that actual uranium oxide particles are highly irregular in shape, with concave surfaces and cavities, we considered two additional large particles: a large 10 μm particle with a closed internal cavity of 4 μm in diameter and height, and a large 10 μm particle with an open cavity of 4 μm in diameter and 7 μm in height. The relevant enhancement factors were also calculated within these cavities assuming that they were filled with ICRU four-element tissue. The closed internal cavity was examined to determine the maximum enhancement factor conceivable, albeit a hypothetical situation. The large particles considered here are about the same size as a typical animal cell, where the nucleus of the cell is usually located roughly in the middle of the cell body. Hence, it is appropriate to determine the enhancement factors within 5 μm of the particles—the so-called dose-scoring region. The dose-scoring region was a layer of constant thickness covering the entire surfaces of each particle. To determine the maximum enhancement, the enhancement factors were also determined for the thinner dose-scoring thickness of 1 μm immediately around the particles. The depth–dose curves for collimated and mono-energetic electron beams show that the dose deposition in a homogeneous material decreases reasonably rapidly and monotonically with distance in the material, owing to the energy-loss straggling and tortuous paths that electrons undergo. For the un-collimated and poly-energetic electrons emerging from a cylindrical uranium particle, and after losing energy passing through the particle into the tissue, the dose deposition would drop off even quicker with distance in the tissue, as would the dose enhancement.

DU particles usually contain some un-oxidized uranium, as combustion on impact is not always complete. Furthermore, DU munitions are constructed from other materials in addition to DU, and DU particles contain a range of other elements depending on the surrounding materials at the time of combustion. Consequently, DU particles contain elements of lower atomic number than uranium (in addition to oxygen), including titanium, aluminium, iron, molybdenum, silicon and calcium (Milodowski 2001; Mitchel & Sunder 2004), which will lower the enhancement effect. Our preliminary investigations revealed that compared with pure uranium, pure uranium oxide (U_3O_8) particles produced enhancement factors that were smaller by about 5–15% for external surfaces and by about 25 per cent for internal cavities; consequently, pure natural uranium was used to maximize the calculated enhancement factors. As the photon/electron cross sections are the same, and the density differences are very small, for the various isotopes of natural uranium, natural uranium is essentially the same as DU. It is interesting to note that the typical human body normally contains about 90 μg of natural uranium, with about 60 per cent located in bones and 40 per cent in soft tissue (ICRP 1975). This mass of uranium is equivalent, hypothetically, to about 750 000 of the small particles being considered, each with an activity of

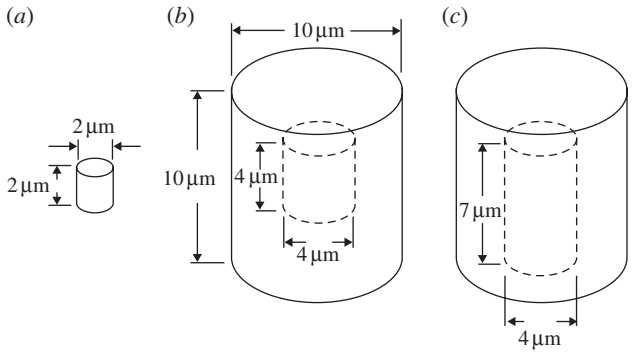

Figure 5. Particle models. (*a*) Small solid particle. (*b*) Large particle with closed cavity. (*c*) Large particle with open cavity. These particles are made of uranium and are surrounded by, and the cavities filled with, ICRU four-element tissue. Particle (*c*) has the same outer dimensions as particle (*b*). The closed cavity in particle (*b*) is centrally located within that particle. The open cavity in particle (*c*) opens at the bottom of the particle shown.

about 1.5 µBq, or about 6000 large particles, each with an activity of about 190 µBq. A recent study by Dorsey *et al.* (2009) found DU in the bodies of only three of 1700 US veterans tested who were exposed to DU munitions, and the exposure histories of these three individuals make it likely that they had retained DU-embedded fragments from previous injuries. Hence, the amount of DU in the bodies of veterans, by either inhalation or ingestion, is considerably smaller than the amount of natural uranium in their bodies.

2.4. Transportation of radiation through the model body

To transport the incident free-in-air gamma-radiation through the model body, we used the Monte Carlo simulation software EGSnrc, an extended and improved version of EGS4 (Kawrakow 2000), with a graphical user interface (Mainegra-Hing 2005).

First, the radial dose distributions across the transverse midplane of the model body, and across two transverse planes located half-way between the midplane and the two ends of the trunk, were calculated using the code DOSrznrc in EGSnrc. This was performed to check that the modelling was satisfactory in giving an estimated effective dose rate that is consistent with the expected effective dose rate due to the natural background gamma-radiation. Ten batches of 300 million histories were accumulated, giving a batch variation of about ± 1 per cent in the estimated doses.

Second, we calculated the doses in the vicinity of the uranium particles, at three positions on the midplane within the body (X in figure 4). Given the very poor geometrical efficiency of our set-up for direct Monte Carlo calculations (i.e. very small particles and scoring regions in a considerably larger body), these calculations were undertaken in two stages using the following five steps.

(i) The incident free-in-air gamma-radiation was transported through the model body without any uranium particles being present. The internal photon and electron fluence-rate spectra were determined, using the code FLUrznrc in EGSnrc, at the three positions where the uranium particles were to be placed in the model body. Ten batches of 300 million histories were accumulated, giving a batch variation of about ± 1 per cent in each energy bin of the estimated internal photon and electron spectra. One hundred, 30 keV wide, energy bins were used covering the range from 0 to 3000 keV.

(ii) Each type of uranium particle, embedded in a large mass of tissue, was then exposed in turn to the internal photon and electron fluence-rate spectra appropriate to the location of the particle in the model body. The doses due to the photon and electron fluences were calculated separately in turn, using the code DOSrznrc, at the various sites around each of the different types of uranium particles. Ten batches of one billion histories were used for calculating the doses due to the photon spectra and 10 batches of 4.5 million histories for calculating the doses due to the electron spectra, each giving a batch variation of about ± 1 per cent. A larger number of histories are required for the photons as they are considerably less interactive than electrons in the body, and most are lost from the body without having any interactions.

(iii) The corresponding photon and electron doses at each site around a particular uranium particle, at a particular position in the model body, were added in their correct proportions with respect to the incident photon and electron fluence-rate spectra to give a total dose at that site.

(iv) Steps (ii) and (iii) were repeated to obtain the total doses at the same sites in tissue without the uranium particles being present.

(v) The enhancement factors were calculated as the ratio (total dose with the uranium particle present)/(total dose without the uranium particle) for each site around each of the types of uranium particles examined, at each of the three positions in the model body. The uncertainties inherent in these calculations were also estimated.

3. RESULTS AND DISCUSSION

The radial dose-rate distribution curve for the midplane is shown in figure 6, along with the average curve for the two planes located half-way between the midplane and the two end planes of the trunk.

The absorbed dose rates just below the surface and on the axis of the trunk are 0.42 and 0.46 mGy yr^{-1}, respectively. The maximum absorbed dose-rate build-up occurs about 1 cm beneath the surface of the trunk, with an absorbed dose rate of 0.54 mGy yr^{-1}. These values compare favourably with the average natural background gamma-radiation dose rate. UNSCEAR (2000) gives the world average effective dose rate, assuming an indoor occupancy of 0.8, as 0.5 mSv yr^{-1}, with a range of 0.3–0.7 mSv yr^{-1}. Hence, the model body and incident gamma-radiation spectrum used in this study are reasonable.

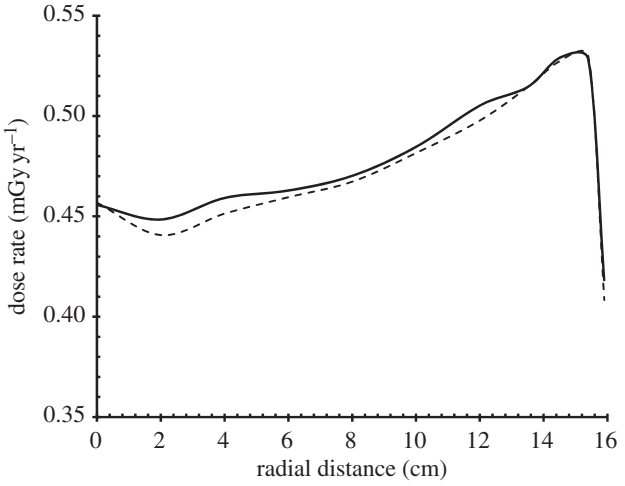

Figure 6. Radial dose-rate distribution across the midplane and half-way planes of the model body due to natural background gamma-radiation. Solid line, midplane; dashed line, average of two half-way planes.

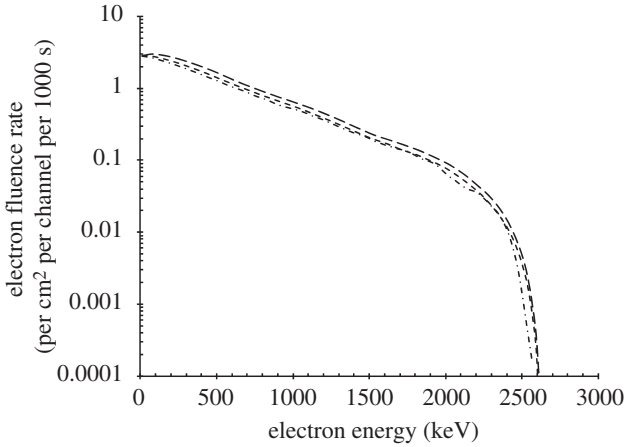

Figure 7. Internal electron fluence-rate spectra. Long-dashed line, just inside body; small-dashed line, half-way inside body; dashed-dotted line, on axis inside body.

The internal photon fluence-rate spectra are shown in figure 3, together with the incident free-in-air gamma-radiation spectrum. The corresponding internal electron fluence-rate spectra are shown in figure 7.

The values of the enhancement factors for the 5 μm dose-scoring region are shown in figure 8*a–c* for the various sites around each type of particle, at each of the three positions in the body. The solid 10 μm particle is not shown because the enhancement factors outside the particle are essentially the same as those for the 10 μm particle with a cavity. The values of the enhancement factors for particles at the position midway between the trunk surface and trunk axis are within the uncertainties of those of the corresponding on-axis cases. Overall, there are no significant differences between the corresponding enhancement factors for the same sites around each of the particle types within a cylindrical volume centrally located within the trunk and with a size of half the trunk radius and half its height. The enhancement factors for the 1 μm dose-scoring regions around the outside of the particles are, on average, about 55 per cent higher than those for the corresponding 5 μm dose-scoring regions.

Although the enhancement factors increase with depth in the body (figure 8), the tissue dose rates without the uranium particles present (figure 6) decrease with depth. Consequently, the dose rates in the vicinity of the uranium particles, being the product of the enhancement factor and the dose rate without a uranium particle present, vary to a lesser degree than do the enhancement factors in terms of the position of the particle in the body. We can now calculate the enhanced dose rates; for example, consider the dose rate received by the 5 μm thick layer next to the flat surface of the 10 μm particle. If this particle were located on the body axis, the enhancement factor would be 2.8 and the dose rate to tissue without the particle present would be 0.46 mGy yr^{-1}, corresponding to a dose rate to tissue with the particle present of 1.3 mGy yr^{-1}. This corresponds in turn to a 'local equivalent dose rate' of 1.3 mSv yr^{-1}, which is less than the figure generally quoted (in terms of effective dose) for the worldwide average radiation dose rate from natural background sources to a whole body. This dose rate is in addition to the equivalent dose rate delivered due to the inherent radioactivity of the uranium particle itself.

The main sources of uncertainty in this study are as follows: the design of the body model (estimated to be approx. ±5%), the design of the model particles (±5%), the approximations used in the EGSnrc code (±5%) and the Monte Carlo transport through the body for each type of radiation (approx. ±1%), giving a statistical uncertainty in the calculation of the enhancement factors of ±2 per cent for the solid large particles, ±3 per cent for the large particles with cavities and ±4 per cent for the small particles, equivalent to ±3 per cent on average for the different particle types. Assuming that the sources of the uncertainties are independent of each other, the final overall uncertainty in the estimated enhancement factors is the square-root of the sum of the various contributing uncertainties squared (Gregory *et al.* 2005)—in this case ±9 per cent. Compared with the natural variability of the shape of the spectrum of the natural background gamma-radiation, which for the five spectra used in this study is ±33 per cent about the average curve, the estimates of the enhancement factors obtained in this study are reasonable, having uncertainties less than the variability of the natural background gamma-radiation spectrum.

The enhancement factors are about 500 times smaller than those proposed by Busby (2005) for similar types of uranium particles; however, the calculation methods differ between the studies, thereby yielding different results. Busby (2005) employed a measured pulse-height spectrum derived from the natural background gamma-radiation and used mono-energetic photon radiation rather than a realistic deconvolved spectrum. Owing to the large over-response of NaI(Tl) to lower energy photons, lower energy pulse events occur much more frequently in scintillation spectra than in the actual free-in-air gamma-radiation spectrum. In the average measured gamma-ray

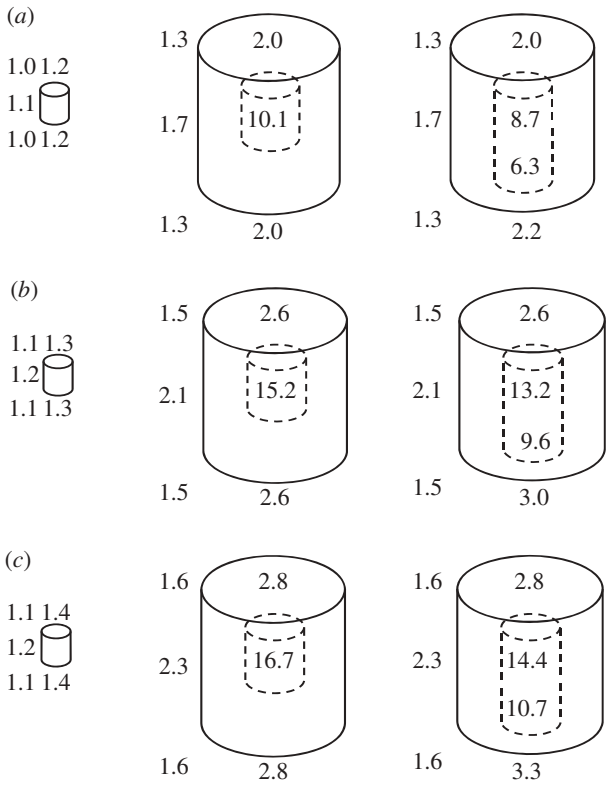

Figure 8. Values of the estimated enhancement factors around uranium particles for the 5 μm dose-scoring region. (*a*) Particles just below the body surface. (*b*) Particles mid-way between the body surface and the body axis. (*c*) Particles on the body axis. The 1 μm size particle is shown on the left, the 10 μm size particle with closed cavity is shown in the centre and the 10 μm size particle with open cavity is shown on the right. The smaller of the two values shown in the open cavity is for the entrance to the open cavity.

spectrum used in the present study, about 60 per cent of the fluence occurs at photon energies below 200 keV, in agreement with Busby (2005); however, after being deconvolved, this value is reduced to about 28 per cent. This is because between 150 keV and 6 MeV, the dominant interaction process for photons in the NaI(Tl) crystal is Compton scattering. Photons scattering with energy in this range have a high probability of leaving the crystal, in which case the energy of the event recorded by the detector is just that of the scattered electron.

The photoelectric effect in the present study is not as prevalent as that assumed by Busby. More importantly, in the present study, the dose at any point near a uranium particle has two contributions: (i) the extra electrons produced in the region of interest by gamma-radiation whether the uranium particle is present or not and (ii) electrons produced outside the region of interest by gamma-radiation that then migrate into the region of interest, again regardless of whether the uranium particle is present. The present approach has enabled us to separately calculate the doses due to these two components. As expected, we found no enhancement of the dose due to the electrons, but the dose was enhanced due to the photons. With no uranium particle present, the dose in the scoring region due to photon absorption was 16 per cent of the total near the surface of the body; on the body axis it was 24 per cent. The dose due to electrons from outside the scoring region makes up the remainder of the dose and is clearly the main component. With the small uranium particle present, the dose in the scoring region due to photon absorption increased to 27 per cent near the surface of the body; on the body axis, it was 41 per cent. The dose due to electrons from outside the scoring region remains the major component. With the large uranium particle present, the dose in the scoring region due to photon absorption increased further to 53 per cent near the surface of the body; on the body axis it was 70 per cent. The situation has now changed: the dose due to photon absorption has become the main component.

The dose contribution due to photon absorption increases by a factor of about 1.4 when progressing from near the body surface to on the body axis. This is expected from the internal photon spectra (figure 3), as the number of low-energy photons increases from the body surface to the body axis. Compared with the small particle, the large particle is more effective in producing photoelectrons by a factor of about 1.8. Self-absorption of the photoelectrons produced in the 10 μm sized particle does not dominate over the production of photoelectrons, meaning that the enhancement factors for these particles are higher than those for the 2 μm sized particles. This finding is contrary to that expected from the estimates of Busby (2005), who proposed that as particles become larger than several micrometres in size, the energy is increasingly reabsorbed within the DU particle, resulting in reduced dose enhancement. The reason for the result obtained in this study is that there is a trade-off between the increase in the production of the photoelectrons within the particle and the decrease in how many pass out of the particle as the particle size increases. A 200 keV photon produces electrons with an average energy of 85 keV, which have a range of about 12 μm in uranium. So uranium particles with sizes around 10 μm should produce a maximum dose-enhancement effect.

4. CONCLUSIONS

The model body used in this study is appropriate in representing the typical adult person exposed to isotropic natural background gamma-radiation. A globally representative natural background gamma-radiation spectrum was used, where the deconvolution from the measured pulse-height spectrum increased the average energy and maximum intensity of the actual photon spectrum, which decreased the amount of enhancement. Finally, the effect of the diffusion of photoelectrons away from the uranium particle was considered, greatly reducing the effect at smaller particle sizes in contrast to results reported by others.

The values of the enhancement factor for the 1 μm sized particle range from 1 to 1.5, while for the 10 μm sized particles the ranges are 1.3–3.3 outside of the particles and 8.7–16.7 inside cavities within

the particles. These are maximum estimates as we have assumed that the particles are pure uranium, natural or depleted, ignoring other lower atomic number materials present in the particles, and that the particles are embedded in soft tissue.

REFERENCES

Aage, H., Korsbech, U., Bargholz, K. & Hovgaard, J. 1999 A new technique for processing airborne gamma ray spectrometry data for mapping low level contaminations. *Appl. Radiat. Isot.* **51**, 651–662. (doi:10.1016/S0969-8043(99)00087-1)

Adam, J.-F., Joubert, A., Biston, M.-C., Charvet, A.-M., Peoc'h, M., Le Bas, J.-F., Balosso, J., Esteve, F. & Elleaume, H. 2006 Prolonged survival of Fischer rats bearing F98 glioma after iodine-enhanced synchrotron stereotactic radiotherapy. *Int. J. Radiat. Oncol. Biol. Phys.* **64**, 603–611. (doi:10.1016/j.ijrobp.2005.09.004)

Berger, M. J. & Hubbell, J. H. 1987 XCOM: photon cross sections on a personal computer. Report NBSIR87-3597. Washington, DC: National Bureau of Standards. See http://physics.nist.gov/PhysRefData/Xcom/Text/XCOM.html.

Biston, M.-C., Joubert, A., Adam, J.-F., Elleaume, H., Bohic, S., Charvet, A.-M., Esteve, F., Foray, N. & Balosso, J. 2004 Cure of Fisher rats bearing radioresistant F98 glioma treated with *cis*-platinum and irradiated with monochromatic synchrotron X-rays. *Cancer Res.* **64**, 2317–2323. (doi:10.1158/0008-5472.CAN-03-3600)

Blum, P., Rabaute, A., Gaudon, P. & Allan, J. 1997 Analysis of natural gamma-ray spectra obtained from sediment cores with the shipboard scintillation detector of the ocean drilling program: example from leg 156. *Proc. of Ocean Drilling Program, scientific results*, vol. 156, pp. 183–195. College Station, TX: Texas A & M University. (doi:10.2973/odp.proc.sr.156.024.1997)

Busby, C. 1998 *The 'second event' theory.* See Low Level Radiation Campaign website www.llrc.org/2ndevent/2ndeventframes.htm.

Busby, C. 2000 Science on trial: on the biological effects and health risks following exposure to aerosols produced by the use of depleted uranium weapons. Occasional Paper 2000/11. Aberystwyth, UK: Green Audit.

Busby, C. 2005 Depleted uranium weapons, metal particles, and radiation dose. *Eur. J. Biol. Bioelectromagnet.* **1**, 82–93.

CERRIE. 2004 *Report of the Committee Examining Radiation Risks of Internal Emitters (CERRIE).* Chilton, UK: National Radiological Protection Board.

Charles, M. W. & Harrison, J. D. 2007 Hot particle dosimetry and radiobiology—past and present. *J. Radiol. Prot.* **27**, A97–A109. (doi:10.1088/0952-4746/27/3A/S11)

Charles, M. W., Mill, A. J. & Darley, P. J. 2003 Carcinogenic risk of hot-particle exposures. *J. Radiol. Prot.* **23**, 5–28. (doi:10.1088/0952-4746/23/1/301)

Cho, W. D., Han, M.-H., Bronson, M. C. & Zundelevich, Y. 2002 Processing of uranium oxide powders in a fluidized-bed reactor. I. Experimental. *J. Nucl. Mater.* **305**, 106–111. (doi:10.1016/S0022-3115(02)01135-2)

Craft, E. S., Abu-Qare, A. W., Flaherty, M. M., Garofolo, M. C., Rincavage, H. L. & Abou-Donia, M. B. 2004 Depleted and natural uranium: chemistry and toxicological effects. *J. Toxicol. Environ. Health—Part B: Crit. Rev.* **7**, 297–317. (doi:10.1080/10937400490452714)

De Stasio, G. *et al.* 2006 Motexafin–gadolinium take up *in vitro* by at least 90% of glioblastoma cell nuclei. *Clin. Cancer Res.* **12**, 206–213. (doi:10.1158/1078-0432.CCR-05-0743)

Dorsey, C. D., Engelhardt, S. M., Squibb, K. S. & McDiarmid, M. A. 2009 Biological monitoring for depleted uranium exposure in U.S. veterans. *Environ. Health Perspect.* **117**, 953–956. (doi:10.1289/ehp.0800413)

DUOB 2007 *Final report of the Depleted Uranium Oversight Board.* Submitted to the Under-Secretary of State for Defence. London, UK: Ministry of Defence.

Edwards, A. A. & Cox, R. 2000 Commentary on the second event theory of Busby. *Int. J. Radiat. Biol.* **76**, 119–125 (including correspondence with C. Busby). (doi:10.1080/095530000139087)

Gregory, K., Bibbo, G. & Pattison, J. E. 2005 A standard approach to measurement uncertainties for scientists and engineers in medicine. *Australas. Phys. Eng. Sci. Med.* **28**, 131–139.

Gustavsson, P., Talbäck, M., Lundin, A., Lagercrantz, B., Gyllestad, P. E. & Fornell, L. 2004 Incidence of cancer among Swedish military and civil personnel involved in UN missions in the Balkans 1989–99. *Occup. Environ. Med.* **61**, 171–173. (doi:10.1136/oem.2002.005538)

Hainfeld, J. F., Dilmanian, F. A., Slatkin, D. N. & Smilowitz, H. M. 2008 Radiotherapy enhancement with gold nanoparticles. *J. Pharm. Pharmacol.* **60**, 977–985. (doi:10.1211/jpp.60.8.0005)

Hamilton, E. I. 1988 The origin, composition and distribution of 'hot particles' derived from the nuclear industry and dispersed in the environment. Department of the Environment Report DOE/RW/88001. London, UK: DoE.

Horn, O., Hull, L., Jones, M., Murphy, D., Browne, T., Fear, N. T., Hotopf, M., Rona, R. J. & Wessely, S. 2006 Is there an Iraq war syndrome? Comparison of the health of UK service personnel after the Gulf and Iraq wars. *Lancet* **367**, 1742–1746. (doi:10.1016/S0140-6736(06)68661-3)

Hugtenburg, R. P., Chaoui, Z. & Pattison, J. E. 2007 Microdosimetric event distributions in sub-cellular volumes with a general purpose Monte Carlo code. *Nucl. Instrum. Methods Phys. Res. A* **580**, 157–160. (doi:10.1016/j.nima.2007.05.057)

ICRP. 1975 *Reference man: anatomical, physiological and metabolic characteristics.* ICRP Publication 23. Oxford, UK: Pergamon.

ICRP. 2003 *Basic anatomical and physiological data for use in radiological protection: reference values.* ICRP Publication 89. Oxford, UK: Pergamon.

ICRU. 1989 *Tissue substitutes in radiation dosimetry and measurement.* ICRU Report 44. Washington, DC: Pergamon.

IOM. 2006 *Gulf War and health: volume 4. Health effects of serving in the Gulf War.* Washington, DC: The National Academies Press.

IOM. 2008 *Gulf War and health: updated literature review of depleted uranium.* Washington, DC: The National Academies Press.

IRC. 2001 *Depleted uranium munitions—comments of the International Committee of the Red Cross.* Geneva, Switzerland: International Red Cross.

Kawrakow, I. 2000 Accurate condensed history Monte Carlo simulation of electron transport: I. EGSnrc, the new EGS4 version. *Med. Phys.* **27**, 485–498. (doi:10.1118/1.598917)

Lowder, W., Beck, H. & Condon, W. 1964 Spectrometric determination of dose rates from natural and fallout gamma-radiation in the United States, 1962–63. *Nature* **4934**, 745–749. (doi:10.1038/202745a0)

Mainegra-Hing, E. 2005 User manual for egs_inprz, a GUI for the NRC RZ user-codes. NRCC report PIRS-801 (Rev A). Ottawa, ON: National Research Council of Canada.

Milodowski, A. E. 2001 A trial investigation by scanning electron microscopy of uranium particulate in building debris

associated with a depleted uranium munitions strike site during the Kosovo conflict. Commercial Report CR/01/145. Keyworth, UK: British Geological Survey.

Mitchel, R. E. & Sunder, S. 2004 Depleted uranium dust from fired munitions: physical, chemical and biological properties. *Health Phys.* **87**, 57–67. (doi:10.1097/00004032-200407000-00007)

Ough, E. A., Lewis, B. J., Andrews, W. S., Bennett, L. G., Hancock, R. G. A. & Scott, K. 2002 An examination of uranium levels in Canadian forces personnel who served in the Gulf War and Kosovo. *Health Phys.* **82**, 527–532. (doi:10.1097/00004032-200204000-00014)

Pattison, J. E., Hugtenburg, R. P., Charles, M. W. & Beddoe, A. H. 2001 Experimental simulation of A-bomb gamma-ray spectra for radiobiology studies. *Radiat. Prot. Dosim.* **95**, 125–136.

Pattison, J. E., Payne, L. C., Hugtenburg, R. P., Charles, M. W. & Beddoe, A. H. 2004 Experimental simulation of A-bomb gamma-radiation: revisited. *Radiat. Prot. Dosim.* **109**, 175–180. (doi:10.1093/rpd/nch320)

Pattison, J. E., Hugtenburg, R. P. & Green, S. 2008 The enhancement of natural background radiation dose around uranium micro-particles. In *Abstracts 12th Int. Congress of the International Radiation Protection Association, Buenos Aires, Argentina, 19–24 October 2008*, p. 179, art. no. 348.

Redus, R., Alioto, M., Sperry, D. & Pantazis, T. 2007 VeriTainer radiation detector for intermodal shipping containers. *Nucl. Instrum. Methods Phys. Res. A* **579**, 384–387. (doi:10.1016/j.nima.2007.04.082)

Royal Society. 2001 *The health hazards of depleted uranium munitions—Part 1.* London, UK: The Royal Society.

Royal Society. 2002 *The health effects of depleted uranium munitions—Part 2.* London, UK: The Royal Society.

Salbu, B., Janssens, K., Lind, O. C., Proost, K., Gijsels, L. & Danesi, P. R. 2005 Oxidation states of uranium in depleted uranium particles from Kuwait. *J Environ. Radioact.* **78**, 125–135. (doi:10.1016/j.jenvrad.2004.04.001)

Sim, M. & Kelsall, H. 2006 Gulf War illness: a view from Australia. *Phil. Trans. R. Soc. B* **361**, 619–626. (doi:10.1098/rstb.2006.1821)

Spiers, F. W. 1949 The influence of energy absorption and electron range on dosage in irradiated bone. *Br. J. Radiol.* **22**, 521–533. (doi:10.1259/0007-1285-22-261-521)

Storm, H. H., Jørgensen, H. O., Kejs, A. M. T. & Engholm, G. 2006 Depleted uranium and cancer in Danish Balkan veterans deployed 1992–2001. *Eur. J. Cancer* **42**, 2355–2358. (doi:10.1016/j.ejca.2006.01.064)

Tickell, O. 2008 How war debris could cause cancer. *New Sci.* **2672**, 8–9. (doi:10.1016/S0262-4079(08)62208-3)

Trueman, E. R., Black, S. & Read, D. 2004 Characterisation of depleted uranium (DU) from an unfired CHARM-3 penetrator. *Sci. Total Environ.* **327**, 337–340. (doi:10.1016/S0048-9697(03)00401-7)

UNSCEAR. 2000 *Sources and effects of ionizing radiations.* Report of the United Nations Scientific Committee on the Effects of Atomic Radiation, vol. I. New York, NY: United Nations Publications.

VADD. 2002 *Combined analysis of the VA and DoD Gulf War clinical evaluation program: a study of the clinical findings from systematic medical examinations of 100,339 US Gulf War veterans.* Washington, DC: Department of Defence.

Waters, L. S. (ed.) 2002 *MCNPX user's manual, version 2.4.0.* Report LA-CP-02-408. Los Alamos, NM: Los Alamos National Laboratory.

WHO. 2001 *Depleted uranium: sources, exposure and health effects.* Geneva, Switzerland: World Health Organization.

Zhang, X. *et al.* 2008 Enhanced radiation sensitivity in prostate cancer by gold-nanoparticles. *Clin. Invest. Med.* **31**, E160–E167.